JACS
JOURNAL OF THE AMERICAN CHEMICAL SOCIETY

ARTICLE

pubs.acs.org/JACS

# Heterogeneous Diffusion in Thin Polymer Films As Observed by High-Temperature Single-Molecule Fluorescence Microscopy

Bente M. I. Flier,[†] Moritz C. Baier,[†] Johannes Huber,[†] Klaus Müllen,[§] Stefan Mecking,[†] Andreas Zumbusch,[†] and Dominik Wöll*[,†,‡]

[†]Fachbereich Chemie, Universität Konstanz, Universitätsstrasse 10, 78464 Konstanz, Germany

[‡]Zukunftskolleg, Universität Konstanz, Universitätsstrasse 10, 78464 Konstanz, Germany

[§]Max-Planck-Institute for Polymer Research, Ackermannweg 10, 55128 Mainz, Germany

Supporting Information

**ABSTRACT:**

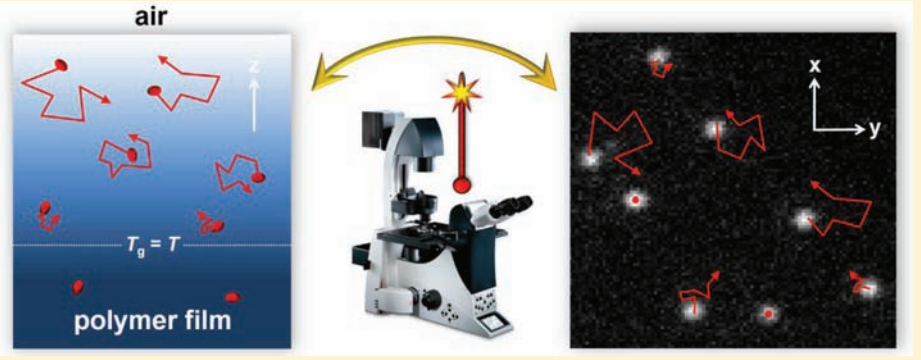


Single-molecule fluorescence microscopy was used to investigate the dynamics of perylene diimide (PDI) molecules in thin supported polystyrene (PS) films at temperatures up to 135 °C. Such high temperatures, so far unreached in single-molecule spectroscopy studies, were achieved using a custom-built setup which allows for restricting the heated mass to a minimum. This enables temperature-dependent single-molecule fluorescence studies of structural dynamics in the temperature range most relevant to the processing and to applications of thermoplastic materials. In order to ensure that polymer chains were relaxed, a molecular weight of 3000 g/mol, clearly below the entanglement length of PS, was chosen. We found significant heterogeneities in the motion of single PDI probe molecules near $T_g$. An analysis of the track radius of the recorded single-probe molecule tracks allowed for a distinction between mobile and immobile molecules. Up to the glass transition temperature in bulk, $T_{g,bulk}$, probe molecules were immobile; at temperatures higher than $T_{g,bulk}$ + 40 K, all probe molecules were mobile. In the range between 0 and 40 K above $T_{g,bulk}$ the fraction of mobile probe molecules strongly depends on film thickness. In 30-nm thin films mobility is observed at lower temperatures than in thick films. The fractions of mobile probe molecules were compared and rationalized using Monte Carlo random walk simulations. Results of these simulations indicate that the observed heterogeneities can be explained by a model which assumes a $T_g$ profile and an increased probability of probe molecules remaining at the surface, both effects caused by a density profile with decreasing polymer density at the polymer−air interface.

## 1. INTRODUCTION

The temperature dependence of the physical properties of polymers is of paramount importance for their application and processing. Therefore, thermal transitions of polymers and in particular the glass transition have been subject to a vast number of studies[1] using different methods such as dielectric spectroscopy,[2,3] magnetic resonance spectroscopy,[4] ellipsometry,[5,6] differential scanning calorimetry,[7] fluorescence spectroscopy,[8,9] small-angle neutron scattering,[10] neutron reflectivity,[11] or combinations thereof.[12] The challenge for all these measurements consists of covering the extended range of length and time scales involved in the phase transitions of polymers. Known methods are normally restricted concerning either their temporal or their spatial resolution, i.e. techniques which can access dynamics detect areas much larger than the molecular scale and thus average over many molecules. In addition, many experimental techniques require specific sample preparation, experimental conditions, or special assumptions for data analysis. Computer simulations for polymer dynamics have also become an important tool, but in contrast to experimental techniques, they are limited to short time intervals and small sample volumes.[13]

**Received:** September 12, 2011
**Published:** November 16, 2011

Single-molecule fluorescence spectroscopy and microscopy (SMS) is a powerful method which can detect dynamics with local resolution close to the molecular scale without averaging or the need for models to extract data.[14−16] Thus, SMS yield valuable information on heterogeneities which together with other techniques and simulations will contribute to an increased understanding of transitions in polymers. Several optical SMS investigations have already been performed to study rotational[17−21] and translational[20,22,23] motion of dye molecules in polymers and glassy liquids. Using highly fluorescent and photostable dyes[24] at low concentrations allowed the resolution of molecule positions with accuracies in the 10 nm range, far below the diffraction limit of optical microscopy.

Single-molecule fluorescence experiments were performed initially at cryogenic temperatures,[25] where single molecules were selectively excited with irradiation into one line of a heterogeneously broadened absorption band. A few years later, use of high numerical aperture microscope objectives allowed the observation of single molecules at room temperature.[26] Today optical single-molecule studies are applied routinely to biological systems at ambient temperature. Especially with respect to material scientific investigations, elevated temperatures are of particular importance, however. The glass transition, crystallization, and melting temperatures of many materials of scientific and practical importance are clearly above ambient temperatures. For example, two of the most common polymers, polystyrene and poly(methyl methacrylate), exhibit bulk glass transition temperatures around 100 °C, too high for single-molecule fluorescence studies to determine structural dynamics around $T_g$. The lack of technical accessibility of such high temperatures limited single-molecule fluorescence studies to polymers with thermal transitions at ambient temperature or below. It also prevented researchers in material sciences from extended investigation of the temperature dependence of single-molecule motion, spectra, anisotropies, etc. These obstacles in establishing SMS as a broader tool for materials science result from the sensitivity of optical lens systems to larger temperature gradients, which can result in disalignment and ultimately ruptures of lens elements.

Here, we report on single-molecule measurements in thin supported polystyrene films of different thicknesses at temperatures up to 135 °C for which we designed a special heating device. We could observe heterogeneities in single-molecule translational diffusion which, in agreement with Monte Carlo Random walk simulations, we attributed to surface effects at the polymer−air interface.

## 2. RESULTS

**2.1. Single-Molecule Fluorescence Microscopy at High Temperatures.** In microscopy of biological samples, physiological temperatures of the sample can be ensured using a heated metal block. However, at higher temperatures this approach can cause severe damage to optical systems which heat up due to thermal radiation from the metal block. In particular at small working distances used for the high numerical aperture objectives in single-molecule measurements, local heating of the sample without transferring too much heat to the objective is required.

We have implemented a high-temperature optical, single-molecule microscope which includes a sample holder for indium tin oxide (ITO)-coated cover glasses (see Figure 1; cf. experimental details in the Supporting Information [SI] for details). These are resistively heated. Thereby, only the sample holder itself attains the desired elevated temperature. Due to its small mass, heat transfer to the optical lens system is limited. In this fashion, sample temperatures up to 200 °C can be reached and held constant at ±0.5 °C. Temperature control is achieved via contactless measurement with an infrared thermometer connected to the power supply of the sample holder. High numerical aperture air objectives allowing single-molecule detection can be used with this setup. For the experiments reported here, we used a homogeneous sample illumination by a 561-nm diode-pumped solid-state laser. The fluorescence of single dye molecules embedded in the polymer film is filtered and imaged on an intensified CCD camera with high quantum efficiency. Movies with varying exposure times are recorded to follow the mobility of single molecules. From the movies, spatiotemporal trajectories are generated and analyzed as outlined below. For the systems studied, beyond a certain temperature dewetting of the film from the glass sample holder was observed. This determined the temperature range of the individual experiments.

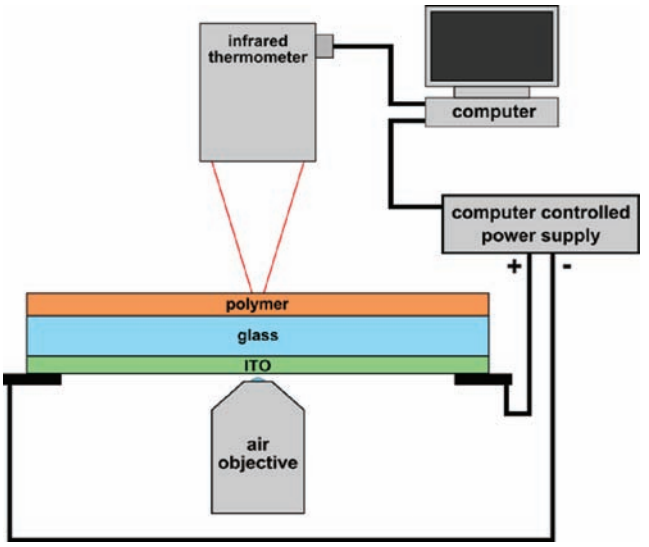


**Figure 1.** Custom-made heating table which allows for heating and temperature control from room temperature up to 200 °C.

The high-temperature single-molecule setup allows us to systematically study the motion of single molecules around the glass transition of a broad variety of polymers with different $T_g$'s. Since so far no experience existed with the performance of dyes in single-molecule experiments at such high temperatures, we chose a perylene diimide derivative[27] (PDI, structure see SI) for our measurements. Perylene diimides show excellent photostability and quantum yield at ambient temperatures,[24] and we could verify that this is also true for temperatures up to 135 °C (see SI).

**2.2. Distinction between Mobile and Immobile Molecules Using Track Radius ($R_g$) Analysis.** The most obvious observation in wide-field movies measured between $T_g$ and 1.1 × $T_g$ was the presence of mobile and immobile molecules in different ratios, i.e. spatial heterogeneities. The distinction between mobile and immobile molecules using step length distribution analysis[28] failed to give satisfactory results due to the fact that immobile molecules showed waggling because of the inaccuracy in the determination of single-molecule positions. We determined the


dx.doi.org/10.1021/ja208581r | J. Am. Chem. Soc. 2012, 134, 480–488

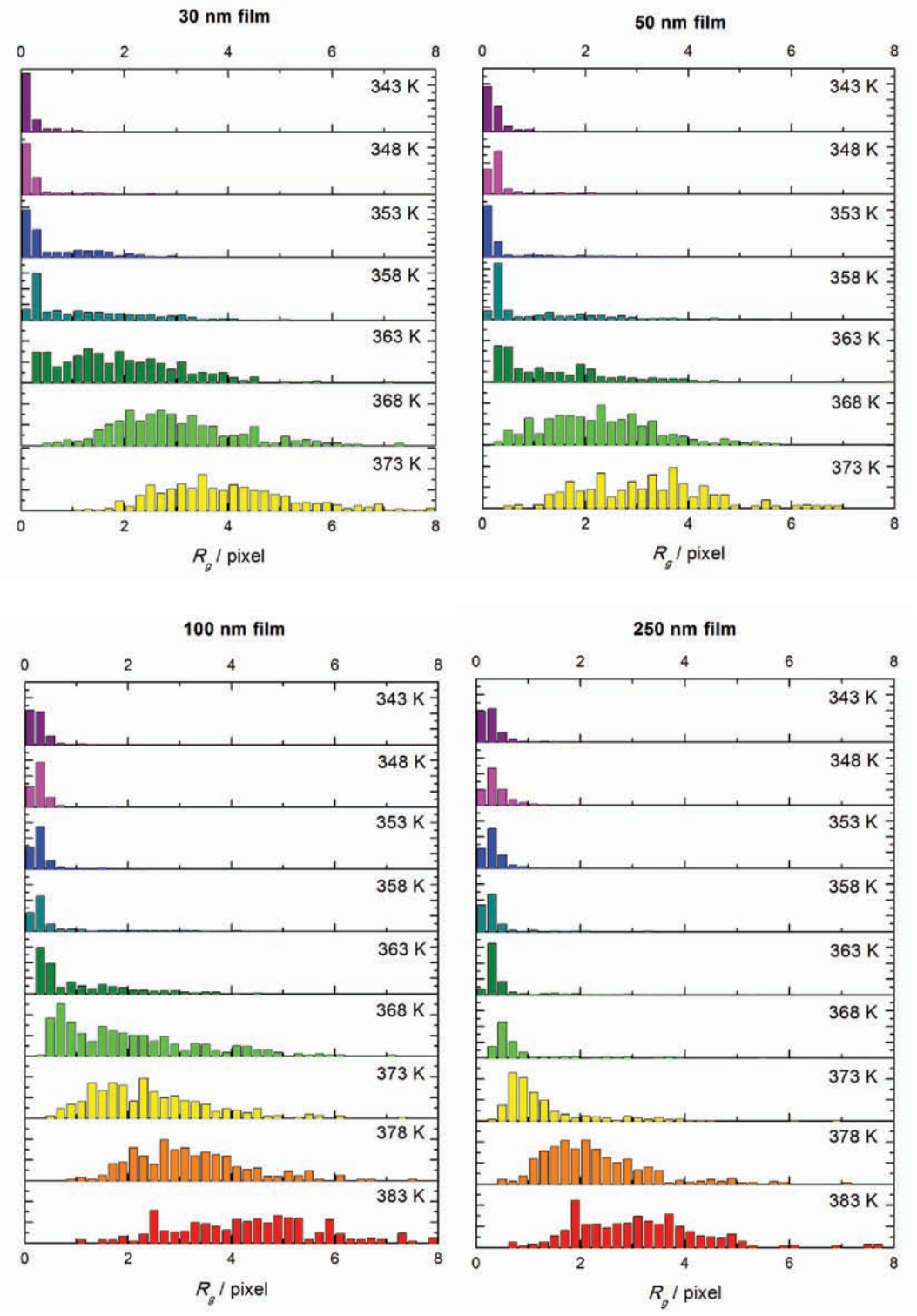


**Figure 2.** Temperature-dependence of the $R_g$ distributions for PS3000 films of different thickness. $R_g$ is given in pixels with one pixel being equivalent to 86 nm. Thirty and 50-nm thin films were not heated higher than 373 K because at higher temperature dewetting effects[33] started to occur. For the histogram of each temperature a number of 160−205 molecules were analyzed.

latter to be 10−15 nm in our experiments (see SI). Very slow or immobile molecules exhibit only a small slope of the mean square displacements for increasing time intervals. Such a small slope, however, is obscured by the noise of the data, and thus, linear fitting of the data points results in extreme inaccuracies in the determination of the diffusion coefficients. We found that a distinction between immobile and mobile molecules is very reliably implemented by an analysis of the track radii $R_g$.[29−31] The molecule positions $x$ and $y$ of each frame are used to calculate the radius of gyration tensor $\hat{T}$

according to

$$\hat{T} = \begin{pmatrix} \frac{1}{N}\sum_{j=1}^{N}(x_j - \langle x\rangle)^2 & \frac{1}{N}\sum_{j=1}^{N}(x_j - \langle x\rangle)(y_j - \langle y\rangle) \\ \frac{1}{N}\sum_{j=1}^{N}(x_j - \langle x\rangle)(y_j - \langle y\rangle) & \frac{1}{N}\sum_{j=1}^{N}(y_j - \langle y\rangle)^2 \end{pmatrix}$$

The square root of the sum of the major and minor eigenvalue $R_1^2$ and $R_2^2$ is the track radius of the corresponding track:

$$R_g = \sqrt{R_1^2 + R_2^2} \cdot \sqrt{\frac{fr_{tot}}{fr_{end} - fr_{start}}}$$

For normal diffusion, $R_g$ grows with the square root of observation time. Thus, in order to compare tracks of different lengths, a correction factor $((fr_{tot})/(fr_{end} - fr_{start}))^{1/2}$ was introduced where $fr_{tot}$ is the overall number of frames, $fr_{end}$ is the number of the last frame and $fr_{start}$ the number of the first frame of the track.

Examples of the positioning of single molecules and a representation of the corresponding $R_g$ values can be found in the movies in the SI. The squared track radius $R_g^2$ of a track is proportional to the area which a molecule probes within a certain time window. For immobile molecules, $R_g$ is small and depends only on the localization accuracy of the molecule which is determined by the signal-to-noise ratio of the detected fluorescence spot. If $R_g$ of a track is significantly larger than the localization-limited $R_g$, the corresponding molecule is defined as mobile. The localization limit for our measurements was set to a value of $R_g$ = 0.6 pixels (52 nm) (see SI), i.e. molecules with $R_g$ < 0.6 pixels are defined as immobile and molecules with $R_g$ > 0.6 pixels as mobile.

Movies of single PDI molecules were recorded in thin PS films ($M_w$ = 3000 g/mol, polydispersity 1.07) at different temperatures. After determination of the molecule positions, their track radii were determined as described above. $R_g$-distributions are presented in Figure 2. Films of 30- and 50-nm thickness were only measured up to 373 K in order to avoid errors in data analysis due to dewetting effects which were observed at higher temperatures. Thick films could be measured up to 408 K (movie presented in SI). At temperatures below 363 K, most molecules show small $R_g$ values below 0.6 pixels and are, according to our definition, immobile. However, it is obvious that a fraction of mobile molecules with higher $R_g$ appears when temperature is raised. In thinner films, a significant fraction of mobile molecules can be observed at lower temperature compared to thicker films. In particular, mobile molecules can be observed at 353 K in 30-nm, 358 K in 50-nm, and 363 K in 100-nm thick films whereas in 250-nm thick films significant motion cannot be observed below 373 K. We assume that the 250-nm film exhibits mainly bulk behavior, whereas the thinner films differ from bulk behavior due to interface-related effects which become more dominant for thinner films. This assumption is in accordance with the observations by Paeng et al.[32] In general, the average $R_g$ increases with decreasing film thickness. However, at low temperatures, where molecules in both thin and thick films are immobile and the determination of $R_g$ is limited by localization accuracy, the distribution of $R_g$ is shifted to slightly higher values in thick films. This shift can be explained by the poorer localization accuracy in the thick films which show more background noise due to fluorescence impurities or Raman scattering. The distribution of the $R_g$ values of mobile molecules is much broader than what would be expected for isotropic diffusion of molecules in a homogeneous medium. In an earlier paper,[23] we have already shown that translational diffusion of mobile molecules is rather heterogeneous in the vicinity of $T_g$, the temperature range also investigated in this work. Only at higher temperatures above ~1.1 × $T_g$ single-molecule diffusion becomes homogeneous.

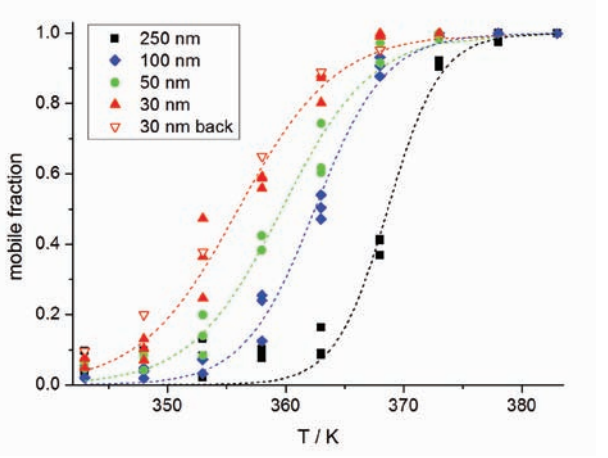


**Figure 3.** Measured fractions of mobile molecules for different temperatures and film thicknesses. For all thicknesses three different movies were analyzed and their mobile fractions plotted to estimate scattering of the data. Data were recorded going from low to high $T$. For 30 nm, data were also recorded during subsequent cooling (open triangles). The lines are a guide to the eyes (according to Boltzmann functions), the derivative of which is shown in Figure 4.

**2.3. Fraction of Immobile and Mobile Molecules.** The fraction $x_{mob}$ of mobile molecules is defined as the number of mobile molecules divided by the overall number of all observed molecules:

$$x_{mob} = \frac{N_{mob}}{N_{mob} + N_{immob}}$$

The dependency of $x_{mob}$ on temperature is plotted in Figure 3 for four different film thicknesses including guides to the eyes which were constructed according to Boltzmann functions $(1 + \exp(T_{1/2} - T)/s))^{-1}$ with the temperature $T_{1/2}$ at which half of the molecules are mobile and the parameter $s$ which is related to the slope of the curve. The temperature $T_{1/2}$ increases with increasing film thickness from 356 to 369 K (see Figure 4 (right)). The change from immobility to mobility is more gradual for thin films than for thick films for which the graph of $x_{mob}$ versus temperature is steeper as represented by the derivatives $dx_{mob}/dT$ which are shown in Figure 4 (left). The derivatives of thicker films reach a higher maximum and are narrower. The latter was quantified using the full width at half-maximum as shown in Figure 4 (right). The observed behavior is not dependent on whether the temperature is approached from low or from high temperatures, as long as no dewetting or other processes, which destroy the film, occur. This was verified for the 30-nm film which was measured from low (343 K) to high (373 K) temperature (filled triangles in Figure 3) and subsequently investigated when decreasing the temperature back to 343 K (open triangles in Figure 3). The data sets show no significant differences.

**2.4. Simulated Fraction of Immobile and Mobile Molecules.** To compare our experimental results with theoretical models, we performed Random Walk Monte Carlo simulations using a customized routine in Matlab. The initial $x$- and $y$-positions (parallel to interfaces) were chosen as the origin, the


dx.doi.org/10.1021/ja208581r | J. Am. Chem. Soc. 2012, 134, 480–488

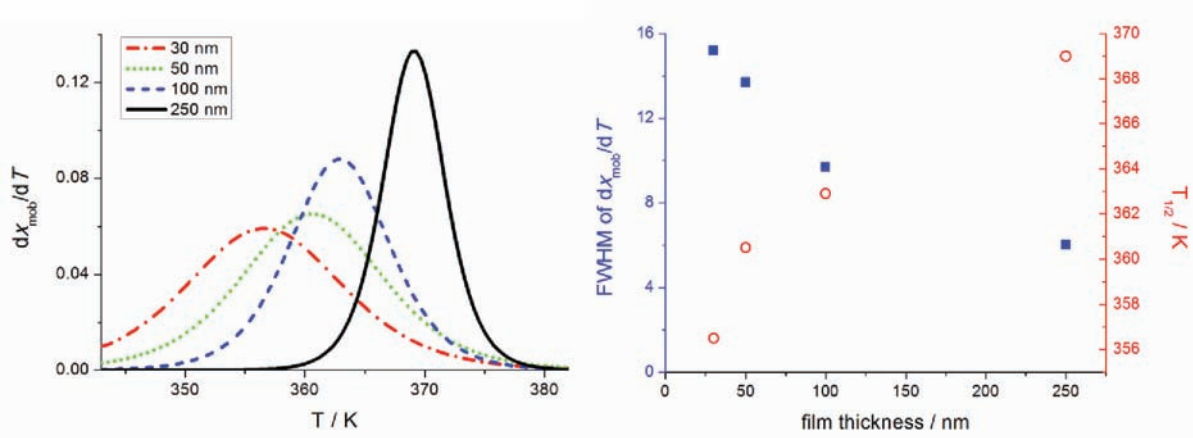


**Figure 4.** (Left) Temperature derivatives of $x_{mob}$ for different film thicknesses. (Right) Dependency of full widths at half-maximum of the corresponding curves and $T_{1/2}$ on film thickness.

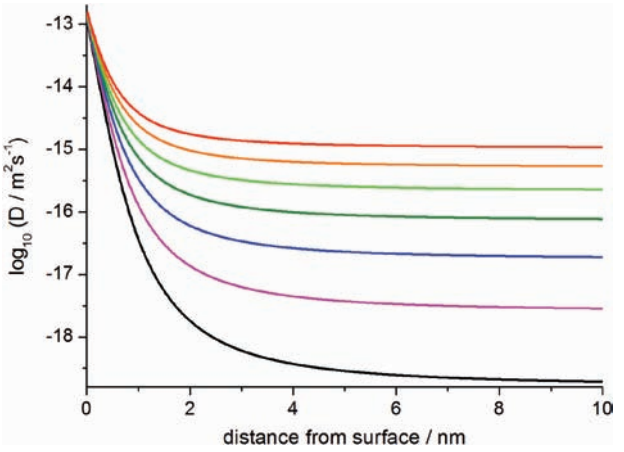


**Figure 5.** Dependence of diffusion coefficient on distance from polymer−air interface for temperatures between 340 K (lowest curve) and 400 K (highest curve) in steps of 10 K.

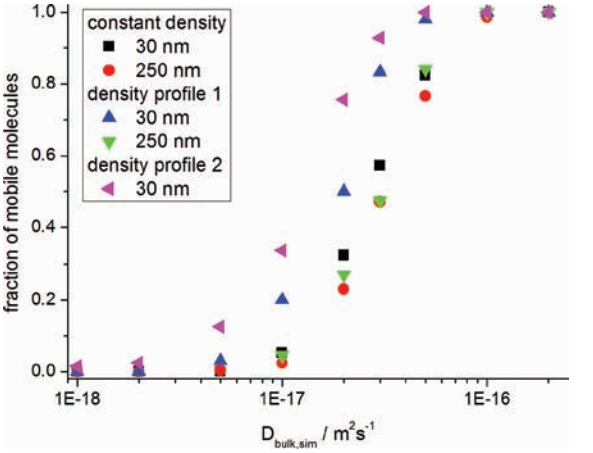


**Figure 6.** Mobile fractions of molecules for simulations of 30- and 250-nm thick films assuming different diffusion coefficients in bulk and $T_g$ profiles as described in the text.

initial $z$-position (perpendicular to interfaces) was randomized between 0 (polymer−air interface) and the film thickness $d$ (polymer−silica glass interface) to simulate an initially equal distribution of dye molecules within the film. In order to account for interfacial effects, a $T_g$-profile as published in literature[34,35] was chosen and the diffusion coefficient profile adapted (see Figure 5 and SI). Interfacial effects were only considered for the polymer−air interface (= surface) which is known to decrease $T_g$. The polymer−glass interface was treated with reflecting boundary conditions since its influence on $T_g$ [36,37] is less pronounced compared to the free surface. In fact, by comparing experimental and simulated data, we verified that the effect of the polymer surface is clearly dominating the influence of the polymer−glass interface (see SI).

The fractions of mobile molecules and their dependence on the diffusion coefficient obtained from the simulations are presented in Figure 6 for film thicknesses 30 and 250 nm, the thinnest and thickest film of our experimental series. For these conditions (red circles and black squares in Figure 6), the mobile fractions differ only in a range of bulk diffusion coefficients between $10^{-17}$ m$^2$ s$^{-1}$ and $10^{-16}$ m$^2$ s$^{-1}$ with the largest difference of ∼0.1 at ∼3 × $10^{-17}$ m$^2$ s$^{-1}$. Each bulk diffusion coefficient can be related to a certain temperature using the Vogel−Fulcher−Tammann equation which allows for a direct comparison of simulated and measured fractions of mobile molecules in films of different thickness.

By comparison to the simulations, the experimentally observed variations between mobile and immobile fractions in the measured films are considerably larger at any temperature. The largest difference can be found at 363 K where the mobile fraction of the 30-nm thin film is 0.8, whereas the one for the 250-nm thick film reaches only 0.1. Thus, our observations cannot simply be explained by random walks of the molecules with a gradient in diffusion coefficients according to the $T_g$ profile used in the simulation. So far, we have only considered that $T_g$ is reduced at the film surface. The cause for this reduction is a decrease of density on the surface. This density profile, however, is also known to cause an increased concentration of small molecules (monomers) at the surface as was shown in simulations by Peter et al.[38] We implemented into our simulations an increased probability for molecules to remain at the surface. Using an increased probability for molecules to remain in the surface


dx.doi.org/10.1021/ja208581r | J. Am. Chem. Soc. 2012, 134, 480–488

layer resulted in a stronger heterogeneity and a larger difference of mobile molecules between thin and thick films which is shown in Figure 6.

## 3. DISCUSSION

**3.1. Explanation for the Observed Heterogeneities.** Single-molecule microscopy allowed us to observe significant heterogeneities in molecular mobility which would be obscured in bulk measurements. It is obvious that these heterogeneities increase significantly with decreasing film thickness when surface effects become more important. We made sure that the heterogeneities observed are not caused by sample preparation since the produced films were heated and dried to remove residual toluene and relax stress prior to measurements. Additionally, to ensure that polymer chains were relaxed, we have chosen polystyrene of low polydispersity and a low molecular weight of 3000 g/mol which is clearly below the entanglement length of PS. Different possibilities which can account for our observations are:

*3.1.1. The Surface Alters the Properties of the Entire Film Causing More Heterogeneities.* Near $T_g$, polymer chains and large molecules do not have enough free volume to move from one position to another. Instead, the space for motion is cleared by another polymer chain which moves to a position which has also become vacant by the chain which occupied it before and so on. This leads to rearranging regions where polymer chains move collectively. Despite many open questions and discussions concerning the glass transition[39,40] this concept originally proposed by Adam and Gibbs[41] is well established. The process at rather long time scales is called $\alpha$-relaxation, in contrast to $\beta$-relaxation which occurs due to the dynamics of polymer segments and chain ends. The length scale of $\beta$-relaxation ($\ll$1 nm) is clearly beyond our observation length scale. The length scale of cooperatively rearranging regions is believed to increase when approaching $T_g$ from higher temperature and has been evaluated between 1 and 4 nm near $T_g$.[42,43] Thus, the heterogeneities observed in our experiments cannot be explained by heterogeneities caused by regions with different dynamics within the film. Molecules which we observe as mobile are at least moving 50 nm and thus already probe several rearranging regions and average over their dynamics. Even though a localization accuracy of 1 nm has been approached using highly fluorescent conjugated polymer nanoparticles,[44] the currently typical localization accuracy for single chromophores does not yet allow for an elucidation of heterogeneity for different cooperatively rearranging regions.

*3.1.2. Heterogeneities Are Due to a $T_g$-Profile at the Surface.* The strong variation of the mobile fractions of single molecules in films of different thickness indicates a significant effect of the interfaces on the mobility of embedded molecules. Such confinement effects[45,46] and their influence on polymer dynamics in thin polymer films are under debate. It has been mostly accepted that, compared to bulk polymers, thin polymer films can exhibit considerable reductions in the glass transition temperature $T_g$[47−49] and their dependence on molecular weight and monomer structure has been investigated.[50] It has also been verified that reduced $T_g$ values are an intrinsic property of the confined material rather than an experimental artifact.[51] However, there are also studies which do not show significant $T_g$ alteration for films as thin as 5 nm (as shown for molecular weights $M_w$ > 25 kg/mol).[12] How much reduction is measured in $T_g$ with decreasing film thickness depends not only on the preparation method, which determines, for example, the amount of remaining solvent in the film and its roughness, but also on the different observables of the methods applied.[48] Most methods such as ellipsometry, dielectric spectroscopy, differential scanning calorimetry, and scattering methods do not offer high spatial resolution and thus measure $T_g$ integrated over the entire film. Simulations, however, show that a reduction in $T_g$ is not caused by the same general reduction for all surface distances within the film, but rather by a drop in $T_g$ at the interfaces. This led to the introduction of a layer model with a highly mobile surface layer existing on top of a less mobile, bulk layer.[47,52,53] The layer model can even be refined to a $T_g$ profile using MD simulations analyzed within mode coupling theory.[35,54] The overall $T_g$ of the film can then be obtained by integration of the $T_g$-profile[35] over the entire film thickness.[34] Such a $T_g$-profile was also obtained using a delayed glassification (DG) model which can predict the effects of molecular weight and film thickness on the film-averaged glass transition for a polystyrene sample[55] and using a percolation of free volume distribution model.[56,57] An experimental approach to determine the length scale of the transition from enhanced dynamics on interfaces to bulk dynamics within polystyrene was presented by Ellison et al.[58] The authors selectively labeled a small layer within the film with pyrene and investigated its dynamics by observing the fluorescence intensity of the film. They observed that the distance over which interfacial effects propagate is much larger than the size of cooperatively rearranging regions which were first claimed by Adam and Gibbs[41] and are believed to be smaller than 5 nm.[59] Ediger and co-workers recently reported fluorescence anisotropy studies in free-standing polystyrene films and estimated a surface layer of 7 nm at $T_g$.[32] A surface mobile layer of less than 2.3 nm was reported for short-chain supported polystyrene films by Yang et al. using temperature-dependent viscosity measurements.[53] A key consideration for all experimental and theoretical analyses is the way in which these methods average $T_g$ values, i.e. how the local $T_g$ values are weighted.[55]

We found that, in thin films, a considerable fraction of mobile molecules is present even at temperatures where no motion can be detected in thick films. Thus, interface effects must play a dominant role for the motion of single molecules. As already pointed out, polymer films show a $T_g$-profile with bulk $T_g$ in the middle of the film and decreasing $T_g$ toward the surface(s). The molecules which are at the polymer−air surface sense a reduced $T_g$ and thus their diffusion coefficient is higher. For thin films, the volume of the surface layer relative to the bulk polymer covers more space, and a higher fraction of mobile molecules can be observed at low temperatures because only dye molecules at the polymer−air interface show significant translational motion. The fraction of mobile molecules becomes larger when the temperature is raised (see Figure 7) since the zone with $T > T_g$ goes deeper into the film.[32] Thus, a distinction between mobile and immobile molecules allows for the investigation of surface effects and, in principle, even of the $T_g$-profile in thin polymer films.

The challenge of resolving differences in molecular mobility along the optical axis lies in the poor $z$-resolution basically inherent to optical microscopy experiments. Since the $z$-resolution of optical single-molecule measurements is above 1 $\mu$m, the $z$-position of molecules in our thin films cannot be resolved. Instead, we observe a projection of all $z$-positions onto the $xy$-plane. Basically, it would be possible to recover information of the depth-dependent $T_g$-profile from the distribution of diffusion coefficients which are assumed to be isotropic in all direction ($x$, $y$, and $z$) but observed as projections onto the $xy$-plane. However, for an exact determination of $T_g$-profiles the localization


dx.doi.org/10.1021/ja208581r | J. Am. Chem. Soc. 2012, 134, 480–488

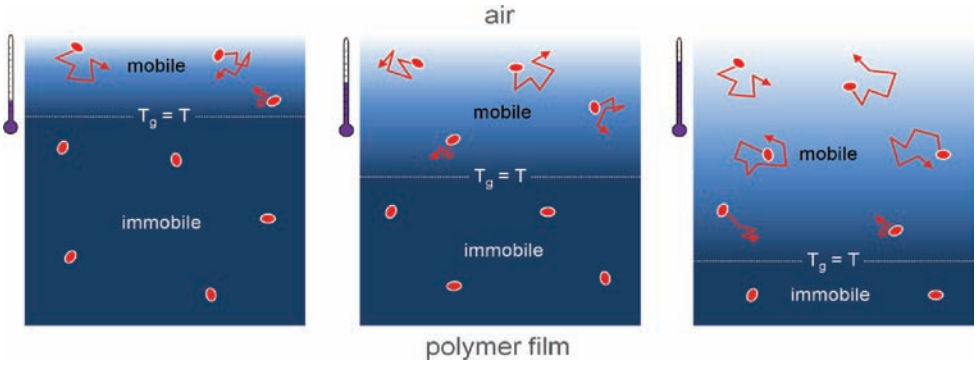


**Figure 7.** Schematic drawing of single-molecule translational motion at the polymer−air interface for increasing temperatures from left to right.

accuracy would have to be in the subnanometer range so that the *z*-position of the probe does not change significantly from one recorded *xy*-position to the next. Otherwise, the diffusion coefficient recorded as *xy*-projections will be averaged over many *z*-positions, and thus the $T_g$-profile will be blurred.

Even though a determination of the exact relationship between *z*-position and diffusion coefficient was not possible, the *xy*-resolution of less than 15 nm allowed us to determine whether reported $T_g$-profiles can account for the observed heterogeneities. At low temperature, the mobility of molecules inside the film is low. Thus, most molecules will not be able to reach the surface where mobility is strongly enhanced as pointed out in the $T_g$-profile shown in Figure 5. However, molecules in the vicinity of the surface will "feel" a lower $T_g$ and thus be able to move significantly. This causes the heterogeneity of single-molecule motion observed especially in thin polymer films ($d$ < 100 nm) where interfaces contribute significantly to polymer dynamics whereas they can be rather neglected in thick films ($d$ > 100 nm).

To put our reasoning on a firmer footing, we performed random walk simulations to check whether our observations can be explained with $T_g$-profiles as stated by the groups of Baschnagel and Herminghaus.[34,35] As obvious from a comparison of Figures 4 and 6, an $R_g$-analysis of our simulated data using $T_g$-profiles shows the correct tendencies but cannot account for the large differences observed for various film thicknesses. This is due to the fact that the localization accuracy is in the same range as the film thickness for thin films, and thus molecules which are mobile probe the entire *z*-space in our simulations and the $T_g$-profile is obscured. Also, reasonable variation of the parameters used for the $T_g$-profile cannot account for the observed heterogeneity. Thus, the comparison between simulation and experiment allows us to exclude that the observed heterogeneity is exclusively due to a $T_g$-profile effect. In simulations, the difference in fractions of mobile molecules between a 30- and a 250-nm film is only 0.1 at most, while it can reach up to 0.8 in the measurements. Such a significant variation cannot be explained by inaccuracies in measurements or imprecise simulation parameters.

*3.1.3. Heterogeneities Are Due to a $T_g$-Profile at the Surface and a Preferred Residence of Dye Molecules in the Less Dense Surface Layer.* In fact, not only $T_g$ but also polymer density is decreased in vicinity to the surface. Thus, it is reasonable to assume that dye molecules which reach the surface area (the first few nanometers) will preferentially remain in this region of lower density. The accumulation of small molecules in the low density surface layer has also been reported by Peter et al.[38] As presented in the Results, we implemented such a behavior into our simulations. It could be shown that using a distribution probability of the dye and applying the $T_g$ profile described above can qualitatively explain our observations. A more quantitative verification of the polymer density profile and its connection to $T_g$ and density probability of the dye distribution is beyond the scope of this work since it would require a more detailed analysis including additional measurements at higher localization accuracy, simulations, and an extensive comparison with other methods. However, the results presented here show the power of single-molecule microscopy to investigate molecular mobility and its heterogeneities in vicinity of thermal transitions in polymers.

**3.2. Why Do We Not Observe Mobility at $T_g$?** Regarding Figure 4 and recalling the $T_g$ of 342 K for PS3000, the question might arise why translational diffusion can only be observed at significantly higher temperatures than $T_g$. In our thickest films, which show mainly bulk behavior, a significant amount of mobile molecules is only found at $T$ > 363 K, ∼25 K above bulk $T_g$. Similar observations have been made by Schob at al. where in PMA ($T_g$ = 281 K) no significant translational motions were detected below 339 K.[20] The reason for the offset between $T_g$ and detectable single-molecule motion is the localization accuracy of single-molecule experiments as will become clear with the following estimation. If, within our observation time of 150 s, a molecule diffuses one pixel (equivalent to 86 nm), its average diffusion coefficient, as calculated using Einstein's formula for the mean square displacement, is approximately $10^{-17}$ m$^2$ s$^{-1}$. Much smaller diffusion coefficients will be obscured by localization inaccuracies. Our simulations in which we set the $R_g$-limit value between immobile and mobile molecules to 0.6 pixel (= 50 nm) show that the diffusion coefficient for which half of the molecules are defined as mobile is $\sim D_{lim} = 3 \times 10^{-17}$ m$^2$ s$^{-1}$ (Figure 6) which is in reasonable agreement with the rough estimation. Applying this value to the Stokes−Einstein equation and assuming a hydrodynamic radius of 1 nm for the PDI dye used we obtain a viscosity $\eta_{lim}$ of $\sim 10^4$ Pa s. This is several orders of magnitudes below $10^{12}$ Pa s, the viscosity which is commonly associated with $T_g$. The temperature $T_{lim}$ at which the viscosity reaches $\eta_{lim}$ can be estimated using the William−Landel−Ferry equation. With the standard parameters $C_1$ = 17, $C_2$ = 50, and $T_0$ = 342 K the value for $T_{lim}$ was calculated to be 385 K. Even though this value is ∼20 K higher than the temperature for which we observe a change from no motion to mobility, it qualitatively rationalizes the offset of translational motion compared to $T_g$. Thus, localization accuracy has to be taken into account when reasoning with translational diffusion of single molecules in the vicinity of $T_g$.


dx.doi.org/10.1021/ja208581r | *J. Am. Chem. Soc.* 2012, 134, 480–488

## 4. CONCLUSION

With the development of a setup which allows for single-molecule microscopy measurements from room temperature to temperatures beyond 100 °C, we establish the possibility to investigate single-molecule dynamics in a temperature range of high practical importance. Thus, single-molecule investigations of the relevant phase transitions of thermoplastic polymers or other materials with elevated glass transition or crystallization temperatures are enabled. We studied the dynamics of single perylene diimide molecules in thin supported PS films of molecular weight 3000 g/mol above their bulk $T_g$. Their motion exhibits significant heterogeneities with a fraction of immobile molecules disappearing gradually with increasing temperature. The amount of immobile molecules also strongly depends on film thickness. In thinner films, molecules become mobile earlier and more gradually. This behavior can be qualitatively explained assuming a surface layer with reduced $T_g$ in which single molecules are able to move faster than in bulk. A comparison of random walk simulations and the results from our measurements however clarifies that a quantitative explanation of our observations is only possible if the concentration of single dye molecules is higher at the film surface than in bulk.

## ■ ASSOCIATED CONTENT

**Supporting Information.** Experimental details, data, and sample movies. This material is available free of charge via the Internet at http://pubs.acs.org.

## ■ AUTHOR INFORMATION

**Corresponding Author**
dominik.woell@uni-konstanz.de

## ■ ACKNOWLEDGMENT

Financial support of the Zukunftskolleg of the University of Konstanz and the Center for Mesoscopic Structures within the Exzellenzinitiative is gratefully acknowledged. We thank Jörg Baschnagel, Matthias Fuchs, and Thomas Voigtmann for valuable discussions and Franziska Rabold for her assistance in tracking single molecules. B.M.I.F. and M.C.B. thank the "Fonds der Chemischen Industrie" for scholarships.

## ■ REFERENCES

(1) Spiess, H. W. *Macromolecules* **2010**, *43*, 5479.
(2) Russell, E. V.; Israeloff, N. E. *Nature* **2000**, *408*, 695.
(3) van den Berg, O.; Sengers, W. G. F.; Jager, W. F.; Picken, S. J.; Wübbenhorst, M. *Macromolecules* **2004**, *37*, 2460.
(4) Heuer, A.; Wilhelm, M.; Zimmermann, H.; Spiess, H. W. *Phys. Rev. Lett.* **1995**, *75*, 2851.
(5) Pye, J. E.; Rohald, K. A.; Baker, E. A.; Roth, C. B. *Macromolecules* **2010**, *43*, 8296.
(6) Campoy-Quiles, M.; Sims, M.; Etchegoin, P. G.; Bradley, D. D. C. *Macromolecules* **2006**, *39*, 7673.
(7) Efremov, M. Y.; Olson, E. A.; Zhang, M.; Zhang, Z. S.; Allen, L. H. *Macromolecules* **2004**, *37*, 4607.
(8) Siekierzycka, J. R.; Hippius, C.; Würthner, F.; Williams, R. M.; Brouwer, A. M. *J. Am. Chem. Soc.* **2010**, *132*, 1240.
(9) Liu, Y. Q.; Haley, J. C.; Deng, K.; Lau, W.; Winnik, M. A. *Macromolecules* **2007**, *40*, 6422.
(10) Schoberth, H. G.; Schmidt, K.; Schindler, K. A.; Böker, A. *Macromolecules* **2009**, *42*, 3433.
(11) Swallen, S. F.; Mapes, M. K.; Kim, Y. S.; McMahon, R. J.; Ediger, M. D.; Satija, S. *J. Chem. Phys.* **2006**, *124*, 184501.
(12) Tress, M.; Erber, M.; Mapesa, E. U.; Huth, H.; Müller, J.; Serghei, A.; Schick, C.; Eichhorn, K. J.; Voit, B.; Kremer, F. *Macromolecules* **2010**, *43*, 9937.
(13) Barrat, J. L.; Baschnagel, J.; Lyulin, A. *Soft Matter* **2010**, *6*, 3430.
(14) Kulzer, F.; Xia, T.; Orrit, M. *Angew. Chem., Int. Ed.* **2010**, *49*, 854.
(15) Wöll, D.; Braeken, E.; Deres, A.; De Schryver, F.; Uji-i, H.; Hofkens, J. *Chem. Soc. Rev.* **2009**, *38*, 313.
(16) Bopp, M. A.; Meixner, A. J.; Tarrach, G.; Zschokke-Gränacher, I.; Novotny, L. *Chem. Phys. Lett.* **1996**, *263*, 721.
(17) Adhikari, S.; Selmke, M.; Cichos, F. *Phys. Chem. Chem. Phys.* **2011**, *13*, 1849.
(18) Zondervan, R.; Kulzer, F.; Berkhout, G. C. G.; Orrit, M. *Proc. Natl. Acad. Sci. U.S.A.* **2007**, *104*, 12628.
(19) Uji-i, H.; Melnikov, S. M.; Deres, A.; Bergamini, G.; De Schryver, F.; Herrmann, A.; Müllen, K.; Enderlein, J.; Hofkens, J. *Polymer* **2006**, *47*, 2511.
(20) Schob, A.; Cichos, F.; Schuster, J.; von Borczyskowski, C. *Eur. Polym. J.* **2004**, *40*, 1019.
(21) Braeken, E.; De Cremer, G.; Marsal, P.; Pepe, G.; Müllen, K.; Vallée, R. A. L. *J. Am. Chem. Soc.* **2009**, *131*, 12201.
(22) Bi, W. G.; Teguh, J. S.; Yeow, E. K. L. *Phys. Rev. Lett.* **2009**, 102.
(23) Flier, B. M. I.; Baier, M.; Huber, J.; Müllen, K.; Mecking, S.; Zumbusch, A.; Wöll, D. *Phys. Chem. Chem. Phys.* **2011**, *13*, 1770.
(24) Weil, T.; Vosch, T.; Hofkens, J.; Peneva, K.; Müllen, K. *Angew. Chem., Int. Ed.* **2010**, *49*, 9068.
(25) Orrit, M.; Bernard, J. *Phys. Rev. Lett.* **1990**, *65*, 2716.
(26) Nie, S. M.; Chiu, D. T.; Zare, R. N. *Science* **1994**, *266*, 1018.
(27) Qu, J. Q.; Zhang, J. Y.; Grimsdale, A. C.; Müllen, K.; Jaiser, F.; Yang, X. H.; Neher, D. *Macromolecules* **2004**, *37*, 8297.
(28) Saxton, M. J. *Biophys. J.* **1997**, *72*, 1744.
(29) Rudnick, J.; Gaspari, G. *Science* **1987**, *237*, 384.
(30) Werley, C. A.; Moerner, W. E. *J. Phys. Chem. B* **2006**, *110*, 18939.
(31) Elliott, L. C. C.; Barhoum, M.; Harris, J. M.; Bohn, P. W. *Phys. Chem. Chem. Phys.* **2011**, *13*, 4326.
(32) Paeng, K.; Swallen, S. F.; Ediger, M. D. *J. Am. Chem. Soc.* **2011**, *133*, 8444.
(33) Reiter, G. *Macromolecules* **1994**, *27*, 3046.
(34) Peter, S.; Meyer, H.; Baschnagel, J.; Seemann, R. *J. Phys.: Condens. Matter* **2007**, *19*, 205119.
(35) Herminghaus, S.; Jacobs, K.; Seemann, R. *Eur. Phys. J. E* **2001**, *5*, 531.
(36) Fryer, D. S.; Peters, R. D.; Kim, E. J.; Tomaszewski, J. E.; de Pablo, J. J.; Nealey, P. F.; White, C. C.; Wu, W. L. *Macromolecules* **2001**, *34*, 5627.
(37) Grohens, Y.; Hamon, L.; Reiter, G.; Soldera, A.; Holl, Y. *Eur. Phys. J. E* **2002**, *8*, 217.
(38) Peter, S.; Meyer, H.; Baschnagel, J. *J. Chem. Phys.* **2009**, *131*, 014902.
(39) Donth, E. *The Glass Transition: Relaxation Dynamics in Liquids and Disordered Materials*; Springer: New York, 2001.
(40) Debenedetti, P. G.; Stillinger, F. H. *Nature* **2001**, *410*, 259.
(41) Adam, G.; Gibbs, J. *J. Chem. Phys.* **1965**, *43*, 139.
(42) Hempel, E.; Hempel, G.; Hensel, A.; Schick, C.; Donth, E. *J. Phys. Chem. B* **2000**, *104*, 2460.
(43) Reinsberg, S. A.; Qiu, X. H.; Wilhelm, M.; Spiess, H. W.; Ediger, M. D. *J. Chem. Phys.* **2001**, *114*, 7299.
(44) Yu, J. B.; Wu, C. F.; Sahu, S. P.; Fernando, L. P.; Szymanski, C.; McNeill, J. *J. Am. Chem. Soc.* **2009**, *131*, 18410.
(45) Napolitano, S.; Wübbenhorst, M. *Nat. Commun.* **2011**, *2*, 260, DOI: 10.1038/ncomms1259.
(46) Jackson, C. L.; McKenna, G. B. *J. Non-Cryst. Solids* **1991**, *131*, 221.
(47) Keddie, J. L.; Jones, R. A. L.; Cory, R. A. *Europhys. Lett.* **1994**, *27*, 59.

(48) Roth, C. B.; Dutcher, J. R. *J. Electroanal. Chem.* **2005**, *584*, 13.
(49) Forrest, J. A.; Dalnoki-Veress, K. *Adv. Colloid Interface Sci.* **2001**, *94*, 167.
(50) Ellison, C. J.; Mundra, M. K.; Torkelson, J. M. *Macromolecules* **2005**, *38*, 1767.
(51) Raegen, A.; Massa, M.; Forrest, J.; Dalnoki-Veress, K. *Eur. Phys. J. E* **2008**, *27*, 375.
(52) Tseng, K. C.; Turro, N. J.; Durning, C. J. *Phys. Rev. E* **2000**, *61*, 1800.
(53) Yang, Z.; Fujii, Y.; Lee, F. K.; Lam, C.-H.; Tsui, O. K. C. *Science* **2010**, *328*, 1676.
(54) Peter, S.; Meyer, H.; Baschnagel, J. *Eur. Phys. J. E* **2009**, *28*, 147.
(55) Lipson, J. E. G.; Milner, S. T. *Macromolecules* **2010**, *43*, 9874.
(56) Merabia, S.; Sotta, P.; Long, D. *Eur. Phys. J. E* **2004**, *15*, 189.
(57) Long, D.; Lequeux, F. *Eur. Phys. J. E* **2001**, *4*, 371.
(58) Ellison, C. J.; Torkelson, J. M. *Nat. Mater.* **2003**, *2*, 695.
(59) Tracht, U.; Wilhelm, M.; Heuer, A.; Feng, H.; Schmidt-Rohr, K.; Spiess, H. W. *Phys. Rev. Lett.* **1998**, *81*, 2727.